B-6

AEC Category: HEALTH AND SAFETY

CEX-65.60

OPERATION HENRE

NEUTRON SPECTROMETRY—OPERATION HENRE (PROGRAM 6)

Robert S. Sanna, James E. McLaughlin,
Arthur Lazanoff, and Keran O'Brien

Issuance Date: November 1969

CIVIL EFFECTS TEST OPERATIONS
U.S. ATOMIC ENERGY COMMISSION

LEGAL NOTICE

Printed in USA. Price ~~$3.00~~. Available from the Clearinghouse for Federal Scientific and Technical Information, National Bureau of Standards, U. S. Department of Commerce, Springfield, Virginia 22151.

USAEC Division of Technical Information Extension, Oak Ridge, Tennessee

NEUTRON SPECTROMETRY–OPERATION HENRE (PROGRAM 6)

By

Robert S. Sanna, James E. McLaughlin,
Arthur Lazanoff, and Keran O'Brien

Approved by:

F. F. Haywood
Technical Director
Operation HENRE
Oak Ridge National Laboratory

L. J. Deal, Chief
Civil Effects Branch
Division of Biology and Medicine
U. S. Atomic Energy Commission

Health and Safety Laboratory
New York Operations Office
U. S. Atomic Energy Commission
April 1969

NOTICE

This report is published in the interest of providing information which may prove of value to the reader in his study of effects data derived principally from nuclear weapons tests and from experiments designed to duplicate various characteristics of nuclear weapons.

This document is based on information available at the time of preparation which may have subsequently been expanded and re-evaluated. Also, in preparing this report for publication, some classified material may have been removed. Users are cautioned to avoid interpretations and conclusions based on unknown or incomplete data.

ABSTRACT

Measurements of neutron spectra with nuclear emulsions at various distances from a 14 MeV neutron source were made at the Nevada Test Site during Operation HENRE. These measurements and supplementary ones made using the neutron-flux integrator developed at the Lawrence Radiation Laboratory, and a version of Bonner's spectrometer, are compared with theoretical calculations. Overall agreement was found to be good.

ACKNOWLEDGMENTS

The authors are indebted to the several persons who undertook the very tedious work of scanning the emulsions, especially our Drexel Institute of Technology students, Terence J. Duff, Harvey J. Armbrecht, and Philip Knorr and our technicians, Salvatore J. Garafalo, Julia Gajzler and Martha Bien. We also wish to acknowledge the necessary assistance at the Nevada Test Site of Fred F. Haywood of ORNL and Zolin G. Burson of E.G.&G., of the HENRE staff, and their associates; and John Dowdall of HASL. Finally, we wish to thank L. D. Y. Ong of HASL for his help in the statistical analyses of our data.

CONTENTS

ILLUSTRATIONS

TABLES

Chapter 1

INTRODUCTION

Operation HENRE at the Nevada Test Site provided us with the opportunity to expose some of our neutron-detection systems near the air ground interface at various distances from a source of 14 MeV neutrons located at various heights above the interface. These exposures were made to measure neutron spectra and fluence as a function of source height and distance. The detector systems used, thick nuclear track emulsions for neutron spectrometry and cobalt flux integrators to determine neutron fluence, were developed for the measurement of neutrons from accelerator shields.[1, 2, 3, 4] Also, a test measurement was made with a version of the Bonner multisphere spectrometer. We anticipated that comparisons of the measurements with theory, as well as with the other HENRE experiments, would be possible.[5, 6]

In this report we describe the detector systems, the experimental plan, and our methods of data analyses, which include improved statistical tests for the acceptance of the emulsion data. Although some comparisons of our results with theoretical calculations are presented, difficulty in reliably achieving high neutron yields prevented the collection of sufficient data to complete our program aims.

REFERENCES

1. K. O'Brien, R. Sanna, and J. E. McLaughlin, "Inference of Accelerator Stray Neutron Spectra from Various Measurements", USAEC Report CONF-651109, 286-305 (1965).

2. J. E. McLaughlin and K. O'Brien, "Accelerator Stray Neutron Dosimetry; Spectra of Low and Intermediate-Energy Neutrons", Neutron Dosimetry, IAEA, Vienna, 335-354 (1967).

3. K. O'Brien, R. Sanna, M. Alberg, J. E. McLaughlin, and S. Rothenberg, "High-Energy Accelerator Shield-Leakage Neutron Spectra", Nucl. Sci. and Eng., 27: 338-347 (1967).

4. A. R. Smith, "A Cobalt Neutron Flux Integrator", Health Phys., 7: 40-47 (1961).

5. "Operation Plan - Operation HENRE", USAEC Report CEX-65.03 (September 1965).

6. R. E. Marshak, "Theory of the Slowing Down of Neutrons by Elastic Collision with Atomic Nuclei", Rev. Mod. Phys., 19: 218-220 (1947).

Chapter 2

EXPERIMENTAL

2.1 DETECTOR SYSTEMS

Three detector systems, to measure neutron spectra (nuclear emulsions and a Bonner multisphere spectrometer) and neutron fluences (cobalt flux integrators), were used during Operation HENRE. A brief description follows.

2.1.1 Nuclear Track Emulsions

We used uncollimated 600 micron thick Ilford G-5 and K-2 nuclear emulsions. Neutrons incident on the emulsion interact with the hydrogen in the gelatin generating recoil protons. The recoil protons leave tracks of silver grains in the emulsion which can be measured with a microscope after development. We use an isothermal development procedure described by Akagi and Lehman[1] and modified by us[2,3] for various thicknesses and types of emulsions.

The developed emulsion pellicles are mounted on glass slides and scanned using our digitized nuclear emulsion microscope. The end points of each track are aligned with an eye piece reticle, and the coordinates of the end points are punched on an IBM card.[3] For Operation HENRE, a sample of approximately 5000 recoil proton tracks was taken and grouped in 0.1 MeV energy intervals to form each acceptable recoil proton spectrum. The neutron spectrum incident on each emulsion was inferred from this proton spectrum using techniques described in section 3.1.

2.1.2 Cobalt Flux Integrators

The cobalt flux integrators are copies of those originally designed by Smith[4] and consist of a 2 in. diameter by $\frac{1}{8}$ in. thick disk of cobalt-59 placed in the center of a cadmium covered 6 in. cylinder of paraffin. The paraffin moderates the fast neutrons which in turn interact with the cobalt to produce ^{60}Co. The cadmium cover serves as a

barrier to thermal neutrons. The ^{60}Co activity of the disk is then measured with a multidimensional gamma-ray spectrometer and the neutron fluence is calculated from a comparison of this activity with that of a standard calibration disk as described in section 3.2.

2.1.3 Bonner Multisphere Spectrometer

We derived a low-resolution, time-averaged neutron spectrum in the energy range of thermal to above 10 MeV with a Bonner-multisphere spectrometer using passive neutron detectors.[5,6] In Operation HENRE we used five polyethylene spheres ranging in diameter from two to twelve inches; each sphere contained paired capsules of ^{6}LiF and ^{7}LiF thermoluminescent detectors (TLD's). To obtain data at low energies we used pairs of bare and cadmium-shielded TLD's. Prior to exposure, samples of both ^{6}LiF and ^{7}LiF TLD's were used for calibration purposes. The TLD's were calibrated by exposing the samples to known doses of monochromatic X-rays.[7] Analysis of the exposed TLD's was done with a modified commercial LiF reader, and the resulting glow curves were then interpreted to get dose per unit area of the curve per milligram of powder. A difference in the reading between the ^{6}LiF and ^{7}LiF TLD's in each of the seven detector channels is a measure of the total thermal neutron density at the center of the detector for the time of the exposure. From these data a neutron spectrum was inferred using the method described in section 3.3.

2.2 EXPERIMENTAL PLAN AND PROCEDURE

Measurements of neutron spectra were to be made near the air-ground interface at various distances from the neutron source with the source at various heights above the ground, using Ilford G-5 and K-2 emulsions. The neutron source was a deuterium accelerator with a tritium target (D-T) to generate 14 MeV neutrons. For identification purposes the accelerator runs were numbered. Seven exposures were planned with the emulsions to be located at distances of 500 meters to 700 meters from the base of the tower supporting the D-T accelerator and with the accelerator at heights ranging from 8.2 meters to 152 meters.[8] The exposures were to be made along a graded area extending from the base of the tower; this area was level out to a distance of about 76 meters and then rose about 30 meters in 1500 meters. Table 2.1 indicates the number of nominal accelerator runs needed to achieve the desired neutron exposure for our emulsions, about $10^{7}n/cm^{2}$. For our purposes, a nominal run is defined as $10^{13}n/sec$ for a 4 hour period.[9]

Our initial participation, during October and November 1966, in Operation HENRE indicated the need to alter our

TABLE 2.1—PROPOSED EMULSION MEASUREMENTS

Source height (meters)	Distance from tower base (meters)	No. of nominal runs needed
8.2	500	2
17	500	2
33	500	2
33	600	4
33	700	9
91	500	2
152	500	4

experimental plan because the neutron yields were found to be less than expected. This lower neutron yield caused us to cancel our exposures at distances greater than 500 meters and to substitute exposures at 100, 200 and 300 meters. We were however able to extend the maximum source height from 152 meters to 343 meters. Also, we had previously decided to use cobalt flux integrators to measure the neutron fluences and to make a measurement of the neutron spectrum using a Bonner multisphere spectrometer as a field test of this detector system. Finally, in November 1968, we participated in an intercomparison with other experimenters. For the intercomparisons, exposures were made at a standard distance of 8.2 meters from the tower with the source at a height of 8.2 meters. The detectors were placed 0.91 meters (3 feet) above the air-ground interface.

Since it was impossible to assume a direction for the incident neutrons, at the source to detector distances (Slant Ranges), the plane wave geometry method of data analyses[10] could not be used in this experiment. It was, therefore, necessary to insure that our emulsions received an isotropic exposure so that we could use our matrix inversion method of analysis.[11]

During the intercomparison we were able to obtain both an isotropic exposure and an edge-normal exposure which approximated plane wave geometry enabling us to use both methods of analysis. To insure an isotropic exposure, the emulsions were rotated about their vertical axis during exposure. We used aluminum tripods to support the emulsion packages. The tripods were secured by tying them to tent stakes driven into the ground. The emulsions were strung on monofilament fish line between the top of the tripod and a lead weight on the ground. The use of small swivels connected between the line and eyelets in the package, left the package free to rotate about its vertical axis and receive the desired isotropic exposure.

TABLE 2.2—EMULSIONS ANALYZED FOR NEUTRON SPECTRA

Source height (meters)	Distance from tower base (meters)	Slant range (meters)	Accelerator run No.'s	Emulsion No.
8.2	8.2	11	*	1040,1037
8.2	200	201	17 to 21	406
8.2	500	503	17 to 21	409
33	200	203	12 to 14	404
91	100	135	26,27	413
91	200	220	26,27	411
152	200	249	48,49	530
343	200	395	43,44	526
343	300	453	28,29	416
343	500	604	28,29	417

*Intercomparison run, November 1, 1968.

The package was also designed to protect the emulsion from the desert heat. At our Laboratory, the emulsion was wrapped in light tight paper, sealed in a plastic envelope and then in aluminum foil. Aluminum foil was used as the outer wrapping because of its low density and heat reflectivity and because its flexibility allowed it to be formed into an airfoil so that the wind would cause it to rotate. Although the background fog on some of our emulsions was higher than normal, no exposures were lost because of heat damage. Some difficulty was encountered with high winds blowing tripods over or tearing the emulsions loose from their moorings. As it is our custom to make duplicate exposures wherever possible, no data were lost.

Table 2.2 lists the emulsions analyzed, grouped according to source height.

The cobalt flux integrators presented no difficulty as far as orientation was concerned, since experiment has shown the detector system to have an isotropic response. Most of the cobalt exposures were made with the integrators on the ground, adjacent to the emulsion tripods. In a few cases the integrators were taped to steel posts at the same height above the ground as the emulsions. The desert heat did pose a problem in that the paraffin in the integrators would soften and weld the two halves of the integrator together. This was overcome by inserting a sheet of mylar film between the two halves of the integrator.

The Bonner multisphere spectrometer test measurement was done for a source height of 91 meters at a distance of 100 meters from the tower base in conjunction with a nuclear emulsion and a cobalt flux integrator. The bare and cadmium covered thermoluminescent powder detectors and the smaller spheres were taped to the legs of the tripod supporting the emulsion package. The larger spheres

and the cobalt flux integrator were arranged on the ground surrounding the tripod. Care was taken to prevent any single detector being shadowed from the neutron source by any other detector. Only one Bonner multisphere spectrometer measurement was attempted, because this system is less sensitive than the emulsions and flux integrators, and the low neutron output of the accelerator made further Bonner multisphere spectrometer measurements impractical. No environmental problems were encountered that affected our Bonner multisphere measurement.

REFERENCES

1. H. Akagi, and R. Lehman, "Neutron Dosimetry in and Around Human Phantom by Use of Nuclear Track Emulsions", Health Phys., 9: 207-220 (1963).

2. R. Sanna, K. O'Brien, M. Alberg, S. Rothenberg, and J. E. McLaughlin, "Nuclear Emulsion Spectrometry at Low and Intermediate Neutron Energies", USAEC Report HASL-162 (July 1964).

3. R. Sanna and J. E. McLaughlin, "Nuclear Emuslion Spectrometry at Low and Intermediate Neutron Energies", USAEC Report HASL-162, Supplement No. 1 (to be published).

4. A. R. Smith, "A Cobalt Neutron Flux Integrator", Health Phys., 7: 40-47 (1961).

5. K. O'Brien, R. Sanna, and J. E. McLaughlin, "Inference of Accelerator Stray Neutron Spectra from Various Measurements", USAEC Report CONF-651109, 286-305 (1965).

6. J. E. McLaughlin and K. O'Brien, "Accelerator Stray Neutron Dosimetry; Spectra of Low and Intermediate-Energy Neutrons", Neutron Dosimetry, IAEA, Vienna 335-354 (1967).

7. A. Shambon, "Determination of Energy Distribution of X-Ray Beams from a 250 kV Constant Potential Machine", USAEC Report HASL-151 (November 1964).

8. "Operation Plan - Operation HENRE", USAEC Report CEX-65.03 (September 1965).

9. F. F. Haywood and J. A. Auxier, "Technical Concept - Operation HENRE", USAEC Report CEX-65.02 (March 1965).

10. H. T. Richards, "A Photographic Plate Spectrum of Neutrons from the Disintegration of Lithium by Deuterons", Phys. Rev., 59: 796-804 (1941).

11. K. O'Brien, R. Sanna, M. Alberg, J. E. McLaughlin, and S. Rothenberg, "High-Energy Accelerator Shield-Leakage Neutron Spectra", Nucl. Sci. and Eng., 27: 338-347 (1967).

Chapter 3

DATA ANALYSIS

3.1 NUCLEAR TRACK EMULSIONS

3.1.1 Derivation of the Neutron Spectrum

Having formed a recoil proton spectrum by measuring the proton track lengths in the emulsion we infer the incident neutron spectrum from this proton spectrum. The proton spectrum is given by

$$P(E_p) = \int_o^\infty \gamma\, \sigma_{n,p}(E_n;E_p) N(E_n) dE_n, \qquad (3.1.1)$$

where $P(E_p)$ is the recoil proton spectrum per cm^3 of emulsion per MeV, γ is the hydrogen atom density of emulsion, $\sigma_{n,p}(E_n;E_p)$ is the differential energy cross section for n-p scattering, and $N(E_n)$ is the neutron spectrum per cm^2 per MeV.

Our method for unfolding the neutron spectrum $N(E_n)$ from equation 3.1.1, an iterative technique of matrix inversion (computer program, HERMES) has been described.[1,2]

We tested the effect of the iterative and smoothing techniques used in the matrix inversion with several known neutron spectra. Recoil proton spectra were calculated from these neutron spectra with equation 3.1.1. These proton spectra were then used as input for HERMES and the calculated neutron spectra thus obtained were compared with the original. Figure 3.1 shows a comparison for a "V" shaped spectrum, composed of a segment where the neutron spectrum is proportional to one over the energy (1/E) in the energy range 0.7 to 5.0 MeV, and a segment where the neutron spectrum is proportional to the energy (E) in the range 5.0 to 20.65 MeV. The bump between 0.75 and 1.1 MeV and the tailing off above 16.0 MeV in our calculated spectrum are believed to be due to the smoothing routine. Since in

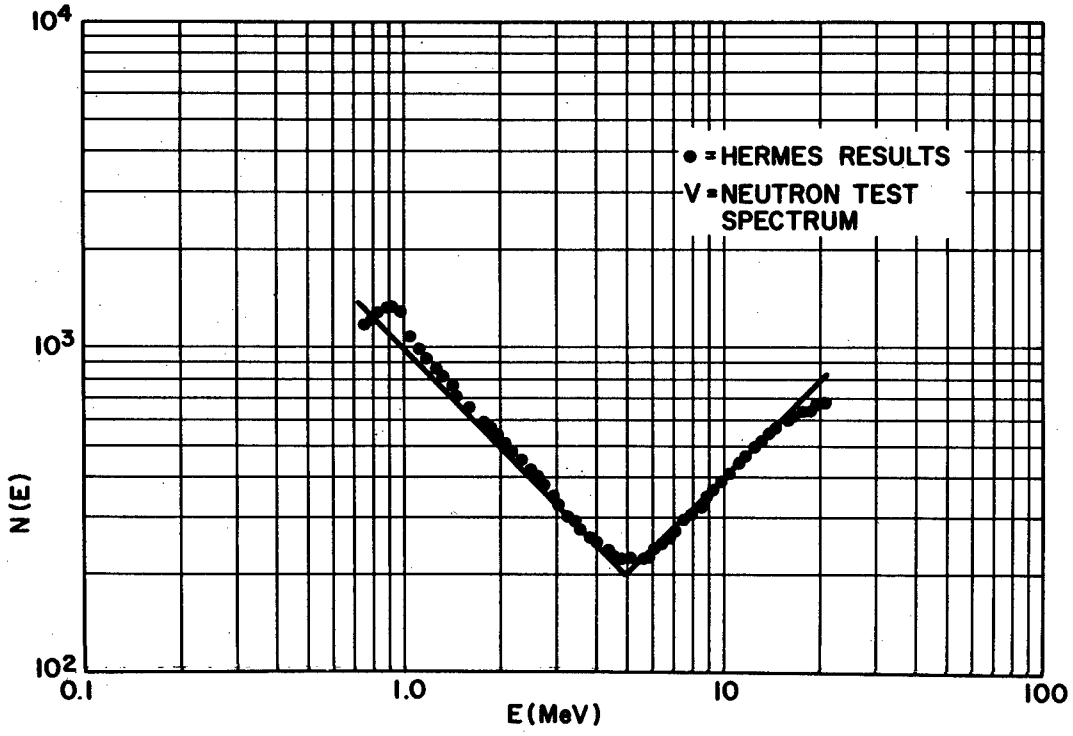

Fig. 3.1—Neutron spectrum obtained by HERMES analysis of proton data generated by a "V" shaped neutron test spectrum.

cases of actual measurement, smoothing is necessary because of statistical fluctuations in the data, the divergences found in Fig. 3.1 are acceptable.

The spectral unfolding program, HERMES, also produces specific neutron dose values for each spectrum. These values depend on the first collision dose factors reported in NBS Handbook 75[3] and by Davis.[4] Recently, Auxier et al[5] and Ritts et al[6] showed that the total tissue KERMA factors for 4- and 11-element tissue approximate those for so-called first-collision dose fairly well.

The specific neutron dose, in terms of rad/(n/cm^2), is computed simply for each measured spectrum from

$$\text{Specific Dose} = \frac{\int_{E_{min}}^{E_{max}} N(E)D(E)dE}{\int_{E_{min}}^{E_{max}} N(E)dE}, \qquad (3.1.2)$$

where D(E) is the appropriate tissue KERMA factor interpolated from Refs. 3 and 4. HERMES also yields specific doses based

on the surface and maximum flux-to-dose data for normal incidence reported by Irving et al.[7]

During the intercomparison run on November 1, 1968, we exposed emulsion at a height of 0.91 meters above the ground and a distance of 8.2 meters from the tower with the source at a height of 8.2 meters above the ground. In addition to exposing a rotating emulsion, which gives us an isotropic exposure, for analysis by HERMES, we obtained an edge-normal exposure which approximates plane-wave geometry. This gave us an independent method of determining the neutron spectrum for comparison with the results obtained from the isotropic exposure.

The neutron energy for plane wave geometry is given by

$$E_n = \frac{E_p}{\cos^2 \theta} , \qquad (3.1.3)$$

where θ is the angle formed in the emulsion by the recoil proton and the incident neutron.[8]

The neutron spectrum, $N(E_n)$, is then obtained from

$$N(E_n) = \frac{P(E_n)}{\gamma \, \sigma_{n,p}(E_n;E_p)} \qquad (3.1.4)$$

where

$P(E_n)$ = corrected proton number at energy E_n (p/cm MeV),

γ = hydrogen atoms per cm^3 of emulsion, and

$\sigma_{n,p}(E_n;E_p)$ = differential energy cross section for hydrogen.[1]

3.1.2 Sources and Estimate of Errors

There are two main sources of error in our nuclear track measurements: gross scanner error and experimental error.

Gross scanner error occurs as a consequence of systematic bias in the determination of a recoil proton track length distribution and is usually observed in the shorter tracks, below about 100 microns, corresponding to about 3.5 MeV protons.[9] It is not possible to correct data for such error; rather, it must be detected and biased data discarded or replaced.

To achieve this, we now employ at least three scanners to measure proton length distributions in different, non-overlapping regions of the same emulsion. If the individual scanner proton spectra obtained in this way are statistically equivalent to the pooled spectrum (the sum of the individual proton spectra), we assume that a valid statistical sample of the track length distribution was obtained in that emulsion. For this test the scanners must record approximately the same number of track lengths or else the pooled spectrum will itself become biased toward the scanner who has the most data. When the data of one scanner fail this test, such data are discarded, replaced, and retested.

The second source, experimental error, has three subclasses, namely in:

1. the determination of the proton track length and its distribution in an emulsion,

2. the conversion and correction of this distribution to a recoil proton energy spectrum, and

3. the derivation of a neutron spectrum from this proton spectrum.

An analysis of the experimental error in our method has been reported.[2] It is quite difficult to follow the error propagation through the involved iterative and smoothing calculations that are used to compute the neutron spectrum. Also, the equation used for the standard deviation in reference 2 relies on a knowledge of the spectral shape and is based on several assumptions.

After trying several methods, we decided that the most practical way to illustrate the uncertainties in neutron spectra was to calculate a set of recoil proton data one standard deviation above and a set one standard deviation below the measured data. These sets of data were then treated as recoil proton spectra from which the neutron spectra were calculated. This resulted in three neutron spectra for each emulsion exposure. One spectrum is for the actual measured proton data; the second is for data one standard deviation above the actual data, and the third is for one standard deviation below the actual data. A plot of these "upper and lower limit neutron spectra" gave us an indication of the statistical reliability of the measurements.

The following approximations to Pearson's[10] confidence limits for a Poisson variable were used to calculate the upper and lower standard deviations at the 68% confidence level.

$$\text{Upper limit} = P(E)*[IP(E) + 0.9 + \sqrt{IP(E) + 0.9}]/IP(E), \quad (3.1.5)$$

$$\text{Lower limit} = P(E)*[IP(E) + 0.01 - \sqrt{IP(E) - 0.31}]/IP(E), \quad (3.1.6)$$

where IP(E) are the uncorrected raw proton data and P(E) is the recoil proton spectrum corrected for the probability that a recoil proton of a given length will escape the emulsion.

The effect of occasional zeroes in individual energy bins of the proton spectrum on the calculation of the upper and lower limits of the neutron spectrum is noteworthy. The standard deviation for zero events in an energy interval is 1.85 for the upper limit and zero for the lower limit. That the lower limit value is identical with the raw data will cause the lower limit neutron spectrum to be closer to the neutron spectrum of the actual data than that of the upper limit. The magnitude of the effect will, of course, depend upon the number of zero count channels in the spectrum.

While these estimates of the errors are probably underestimates, we feel that at this time they give us the best values we can obtain.

3.2 COBALT FLUX INTEGRATORS

3.2.1 Obtaining the Neutron Fluence

As previously mentioned in section 2.1.2 the activity of the ^{60}Co present in the disk being analyzed when compared with the activity of a calibration disk enabled us to compute the neutron fluence to which the cobalt flux integrator had been exposed. In this report, we are discussing neutron fluences measured during Operation HENRE and we will, therefore, refer to the disk being analyzed as the HENRE disk and the neutron spectrum to which it was exposed as the HENRE spectrum.

The most critical part of the determination of the neutron fluence is the accurate measurement of the cobalt-60 activity in the HENRE and in the calibration disks. Since the count rates can be very low, it is necessary to count the disks on a system that has a very low background. Cobalt-60 emits two coincident gamma-rays with energies of 1.17 and 1.33 MeV, thus we were able to use a multi-dimensional coincident gamma-ray spectrometer.[11] The exposed cobalt disk was mounted between two 20 cm x 10 cm NaI(Tl) crystals, enclosed in a large, cylindrical, plastic phosphor, anticoincidence shield. Only those events which occurred in coincidence in the two primary crystals and were not detected by the anticoincidence shield are recorded in the 4096 channel analyzer. This combination of coincident counting and anticoincidence shielding reduces the background by a factor of about 200.[11]

The cobalt flux integrator has been shown to have an approximately constant response with energy, based on measurements down to about 0.4 MeV.[12] Usually, account is not taken of the effect of the relative energy response of the cobalt flux integrator to the spectrum of the calibration source or the HENRE source. In order to develop an energy response for the entire energy range, we employed the calculated data for Bonner spheres reported by McGuire[13]. We assumed the cobalt flux integrator to be approximated by a sphere with a 6.9 in. diameter, and that the cobalt and LiF responses to neutrons were the same. The Bonner sphere data were corrected to account for the 0.07 cm. cadmium covering on the integrator. Using the Gregory-Newton interpolation formulae,[14] the responses of the 2 in., 5 in., and 8 in. Bonner spheres were then used to interpolate the cobalt flux integrator response function, RF(E).[15] The resulting response agreed as well as can be expected with Smith's data.

The response R of the cobalt flux integrator is then given by

$$R = \frac{\int_{E_{min}}^{E_{max}} N(E)\,RF(E)\,dE}{\int_{E_{min}}^{E_{max}} N(E)\,dE} \qquad (3.2.1)$$

where N(E) is the neutron spectrum to which it has been exposed.

To calculate the response R for the calibration disk, which was exposed to our 10 curie Pu-Be source, we used the spectrum we measured with emulsion,[9] and for the HENRE spectra we used those calculated by Straker[16] for the appropriate slant range. Plotting the response "R" for Straker's spectra versus slant range (g/cm^2) we interpolated the values of R for the appropriate slant ranges of the cobalt flux integrator exposures. The interpolation was done with the range expressed in units of g/cm^2 to correct for the difference in the air density used in Straker's calculations (1.11 x 10^{-3} g/cm^3) and that measured at the test site during Operation HENRE (1.00 to 1.08 x 10^{-3} g/cm^3).

Having determined the response of the cobalt flux integrator to the appropriate neutron spectrum and having measured the activity of the ^{60}Co in the HENRE disk and the calibration disk the neutron fluence, F_H, is calculated using the equation

$$F_H = \frac{C_H W_C R_C}{C_C W_H R_H} \times EXP\left[\lambda T_C - \lambda \frac{(T_{H_1} + T_{H_2})}{2}\right] \times F_C \qquad (3.2.2)$$

where

C_H = count of the HENRE disk, corrected for background
W_H = mass of the HENRE disk
C_C = count rate of the calibration disk, corrected for background
W_C = mass of the calibration disk
R_C = response of the cobalt flux integrator to the neutron spectrum of the calibration source from equation 3.2.1
R_H = response of the cobalt flux integrator to the HENRE neutron spectrum from equation 3.2.1
T_C = date of exposure of the calibration disk
T_{H_1} = starting date of the exposure to the HENRE source
T_{H_2} = ending date of the exposure to the HENRE source
λ = decay constant for cobalt-60 = (0.69315/5.24) years^{-1}
F_C = neutron fluence to which calibration disk was exposed.

The relationship in Equation (3.2.2) holds when the time lapse between counting the HENRE disk and counting the calibration disk is small compared to the half life of ^{60}Co.

3.2.2 Error Propagation

There are several sources of error in our determination of the neutron fluence with the cobalt flux integrator. First, there is the counting statistics which are reported with the count rates as the standard deviation at the 90% confidence level. This error is followed through the calculation of the neutron fluence. It varied from about 2.5 to 14% depending on the activity of the HENRE disks. To test the counting precision for ^{60}Co of the multidimensional analyzer, one of our calibration foils was counted several times over a period of months and the precision error calculated. This error was found to be about 6.5%. The error in the calibration of our 10 curie Pu-Be neutron source which was used to irradiate our calibration disk is 1.6% as reported to us by NBS. The overall error due to accuracy, precision, and calibration, results in errors in the measurement of HENRE neutron fluence on the order of 7-15%. We must also consider, when normalizing our data to unit source neutrons, using source output figures calculated from sulfur pellet activation, the error in the source output data. This error is estimated to be about 5%.

3.3 BONNER SPECTROMETRY

We also made a single exposure of the Bonner multisphere spectrometer during Operation HENRE to test its capability to make field measurements of neutron spectra. We described the spectrometer and the method of data readout in section 2.1.3.

The data thus obtained from the TLD's in the various spheres and in the bare and cadmium-covered capsules are unfolded, using a 7 x 52 response matrix developed from data computed at Los Alamos using transport calculations, to obtain a neutron spectrum.[1, 2, 13] In this unfolding method, we assume a smooth non-negative spectrum, and iteratively compute the readings of the TLD's until the computed values converge to the measurements.

The energy resolution of the Bonner spectrometer is poor and there is no simple way of expressing it as it depends upon the neutron spectrum. We have not yet studied the error propagation for the Bonner spectrometer system and therefore will not attempt to estimate the errors in our measurement.

REFERENCES

1. K. O'Brien, R. Sanna, and J. E. McLaughlin, "Inference of Accelerator Stray Neutron Spectra from Various Measurements", USAEC Report CONF-651109, 286-305 (1965).

2. K. O'Brien, R. Sanna, M. Alberg, J. E. McLaughlin, and S. Rothenberg, "High-Energy Accelerator Shield-Leakage Neutron Spectra", Nucl. Sci. and Eng., 27: 338-347 (1967).

3. Measurement of Absorbed Dose of Neutrons, and of Mixtures of Neutrons and Gamma Rays, Handbook 75, National Bureau of Standards (1961).

4. F. J. Davis, "Neutron Dose Determinations with Threshold Detectors", Selected Topics in Radiation Dosimetry, Proceedings of the Symposium on Selected Topics in Radiation Dosimetry, IAEA, Vienna (1960).

5. J. A. Auxier, Health Physics Division Annual Progress Report, USAEC Report ORNL-4168, 223-225 (October 1967).

6. J. J. Ritts, E. Solomito, and P. N. Stevens, "Calculations of Neutron Fluence-to-KERMA Factors for the Human Body", USAEC Report ORNL-TM-2079 (January 1968).

7. D. C. Irving, R. G. Alsmiller Jr., and H. S. Moran, "Tissue Current-to-Dose Conversion Factors for Neutrons with Energies from 0.5 to 60 MeV", USAEC Report ORNL-4032 (1967).

8. R. Sanna, K. O'Brien, M. Alberg, S. Rothenberg, and J. E. McLaughlin, "Nuclear Emulsion Spectrometry at Low and Intermediate Neutron Energies", USAEC Report HASL-162 (July 1964).

9. R. Sanna and J. E. McLaughlin, "Nuclear Emulsion Spectrometry at Low and Intermediate Neutron Energies", USAEC Report HASL-162, Supplement No. 1 (to be published).

10. E. S. Pearson and H. O. Hartley, "Biometrika Tables for Statisticians", University Press, Cambridge (1954).

11. C. G. Sanderson, "Determination of ^{226}Ra and ^{228}Th in Food, Soil, and Biological Ash by Multidimensional Coincident Gamma-Ray Spectrometry", Health Phys. (in press).

12. A. R. Smith, "A Cobalt Neutron Flux Integrator", Health Phys., 7: 40-47 (1961).

13. S. A. McGuire, "Dose Monitoring Instrument for Neutrons for Thermal to 100 MeV", USAEC Report LA-3435 (1966).

14. I. S. Sokolnikoff and R. M. Redheffer, "Mathematics of Physics and Modern Engineering", McGraw Hill, New York, Toronto and London, p. 697 (1958).

15. A. S. Lazanoff and J. E. McLaughlin, "Feasibility Study on Use of LiF Detectors in Neutron Flux Integrators", USAEC Report HASL-206 (March 1969).

16. E. A. Straker, "Time-Dependent Neutron and Secondary Gamma-Ray Transport in an Air-Over Ground Geometry, Volume II, Tabulated Data", USAEC Report No. ORNL-4289, Vol. II (September 1968).

Chapter 4

RESULTS

4.1 NUCLEAR TRACK EMULSIONS

The "upper and lower limit" neutron spectra from ten emulsion exposures are shown in Figs. 4.1 through 4.10. The specific tissue doses obtained from these spectra are listed in Table 4.1 as a function of slant range. Although low source output prevented us from making the measurements we originally planned, we were able to compare some of our measured spectra with theoretical results. For comparison purposes all neutron spectra were normalized to unit area.

Figures 4.1, 4.2 and 4.3 show our measured spectra compared with the calculated spectra of Straker[1] for a source height of 54 feet and similar slant ranges. In Figs. 4.2 and 4.3 we show peaks at about 1.5 MeV which do not appear in the theoretical spectra. We believe these peaks to be due to D-D neutrons. One should also note the inflection in our data at about 2.5 MeV where Straker shows a peak between 2.35 and 2.46 MeV, due to the minimum in the total cross section for oxygen at 2.37 MeV.[2] The emulsion spectrometer cannot resolve this peak although the inflections in our data indicate its existence. The minima between 8 and 10 MeV in the theoretical spectra, also, are not resolved because of the low resolution of the emulsion spectrometer.[3]

In Fig. 4.4 we compare our measured spectrum with the homogeneous medium Monte Carlo calculations for the same slant range of Yampol'skii, et al.[4] Also shown is the calculated spectrum of Mittelman for a source height of 80 meters and a distance of 500 meters.[5] Although the conditions of Mittelman's calculation are not the same as our measurement (his distance being 500 meters instead of 200 meters and his source height, 80 meters instead of 91 meters) the comparison is of interest. On the whole the agreement is good except for a minimum in Mittelman's data at 12.5 MeV which we do not detect because of our resolution, about 50%. Once again we show a 1.5 MeV peak and an inflection

at about 2.2 MeV due to D-D neutrons and the 2.37 MeV peak caused by the oxygen cross section minimum.

In Fig. 4.5 we again display the Yampol'skii data for the same slant range as our emulsion spectrum; again the agreement is as good as can be expected.

Figure 4.6 shows a comparison between edge-on (#1040) and rotating (#1037) emulsions, exposed during the intercomparison experiment on November 1, 1968. Emulsion #1040 was analyzed by HERMES and by the plane wave method of analysis. As one can see the error bars on the plane wave points are quite large. This is due to the collimation effect of accepting only those recoil protons which fall within a 20^{o} half angle acceptance cone. In scanning

TABLE 4.1—SPECIFIC TISSUE DOSE FROM EMULSION SPECTRA

Slant range (meters)	Source height (meters)	Distance from tower base (meters)	Emulsion No.	Specific dose 1st Collision Surface ($\times 10^{-9}$ rads/n/cm^2)		Maximum
11	8.2	8.2	1040 (HERMES)	4.9±0.3	6.3±0.3	6.8±0.3
11	8.2	8.2	1040 (WAVE)	4.8±0.2	6.5±0.2	6.5±0.2
11	8.2	8.2	1037 (HERMES)	4.7±0.3	6.1±0.3	6.6±0.4
135	91	100	413 "	4.9±0.3	5.2±0.4	5.5±0.4
201	8.2	200	406 "	4.3±0.3	5.6±0.4	6.0±0.5
203	33	200	404 "	4.5±0.4	5.8±0.5	6.3±0.6
220	91	200	411 "	4.2±0.3	5.5±0.3	5.9±0.3
249	152	200	530 "	4.5±0.4	5.9±0.5	6.3±0.6
395	343	200	526 "	4.3±0.5	5.6±0.6	6.0±0.7
453	343	300	416 "	4.3±0.4	5.6±0.5	5.9±0.6
503	8.2	500	409 "	4.1±0.4	5.4±0.5	5.7±0.5
604	343	500	417 "	2.9±0.7	3.9±0.7	4.0±1.0

emulsion #1040, 14,867 tracks were recorded, of these 1600 fell within the acceptance angle. However, 722 of these 1600 tracks were below 0.7 MeV, the minimum energy for our emulsion spectrometer. This left us with but 878 tracks to construct our spectrum, so naturally the statistics are poor. The agreement between emulsions #1040 and 1037 as analyzed by HERMES is good and considering the poor statistics so is the agreement as analyzed by the plane wave method. The specific tissue doses listed in Table 4.1 calculated for the three spectra are in good agreement.

In Figs. 4.7 through 4.10 we show other spectra measured during HENRE. These spectra were not compared with theoretical spectra. It should be noted that emulsion #413 in Fig. 4.7 was damaged during development and the data are suspect.

(Text continues on page 34.)

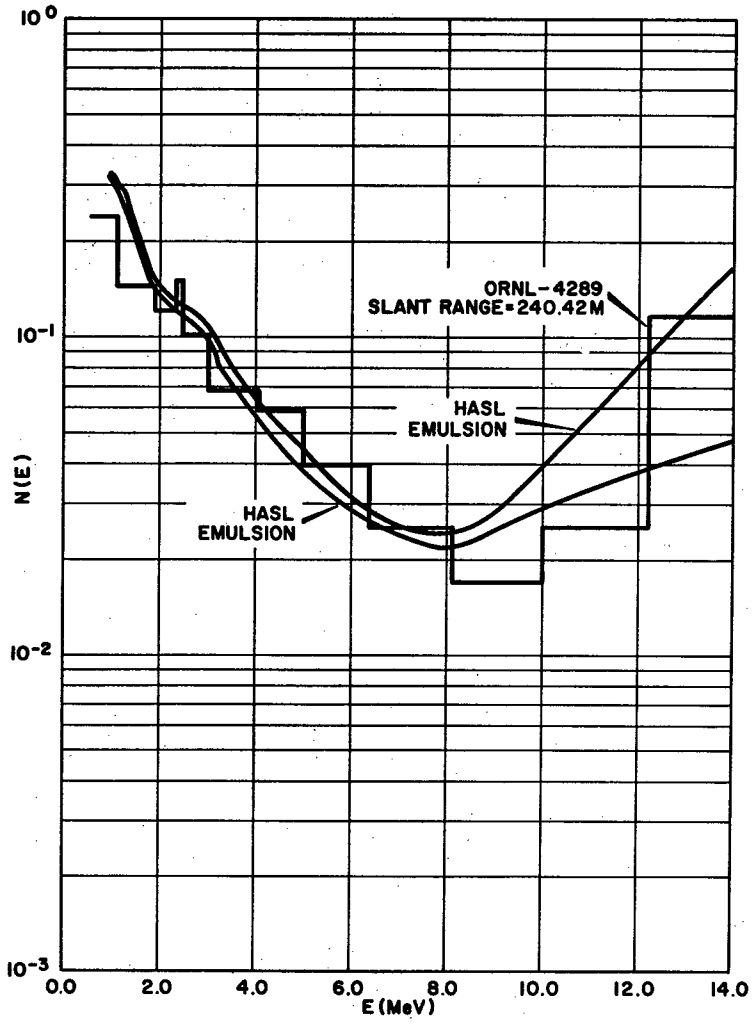

Fig. 4.1—Neutron spectrum, Emulsion # 406 (source height = 8.2 m, distance = 200 m, slant range = 201 m), compared with Straker's calculations (ORNL).

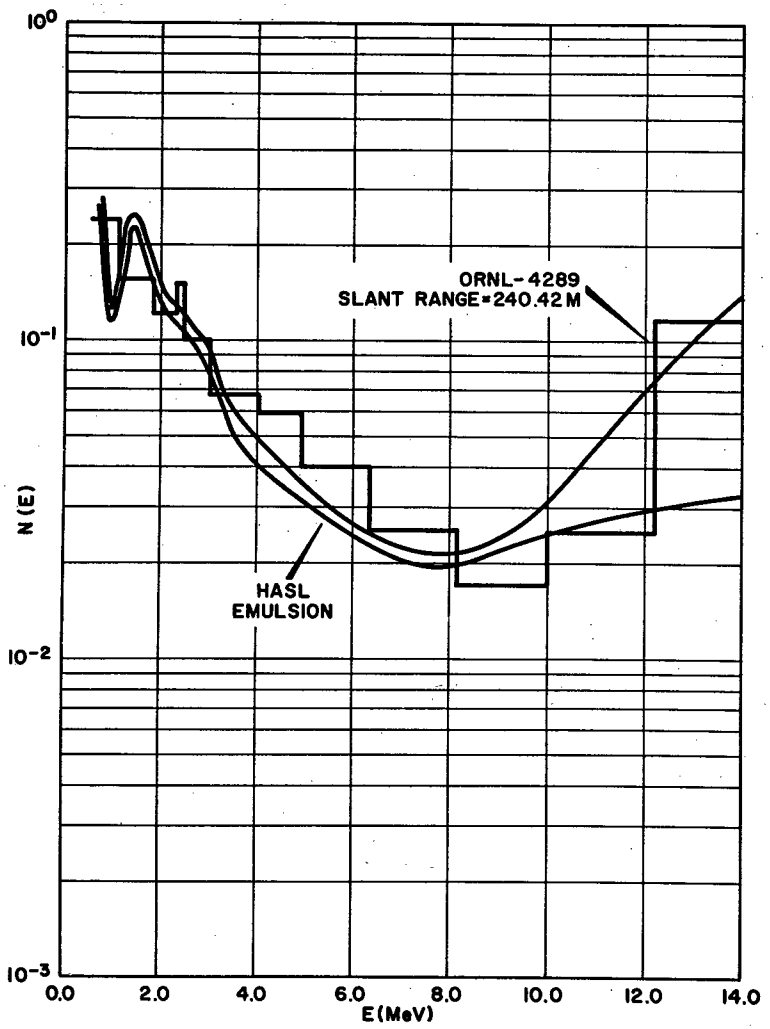

Fig. 4.2—Neutron spectrum, Emulsion # 404 (source height = 33 m, distance = 200 m, slant range = 203 m), compared with Straker's calculations (ORNL).

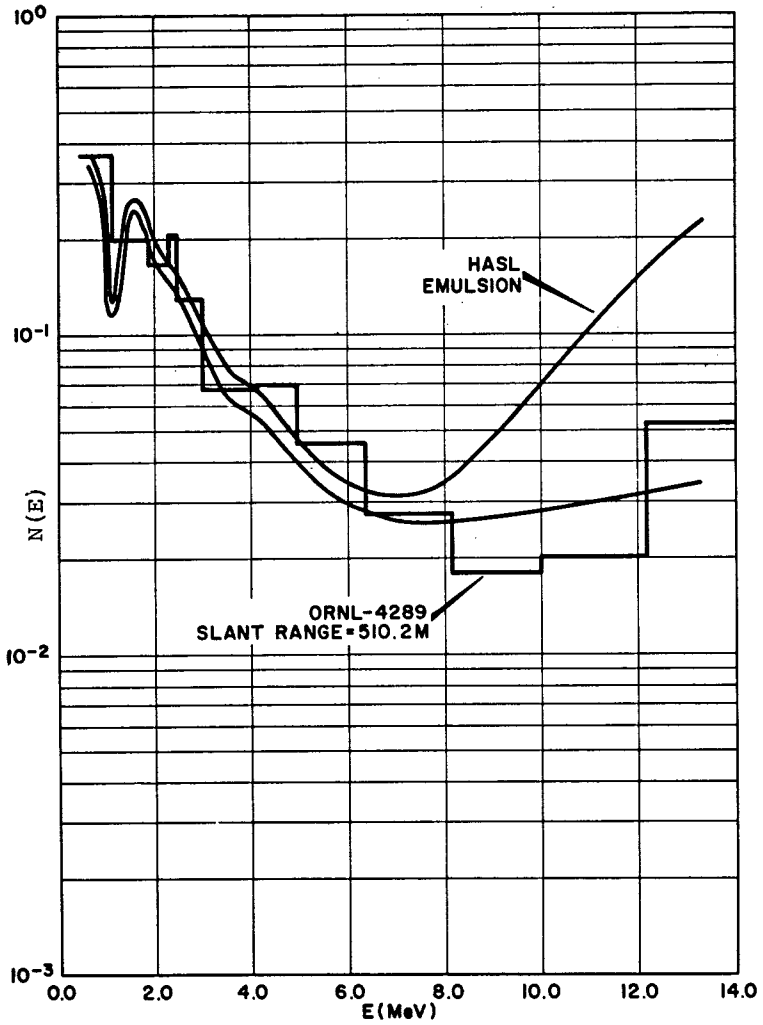

Fig. 4.3—Neutron spectrum, Emulsion # 409 (source height = 8.2 m, distance = 500 m, slant range = 503 m), compared with Straker's calculations (ORNL).

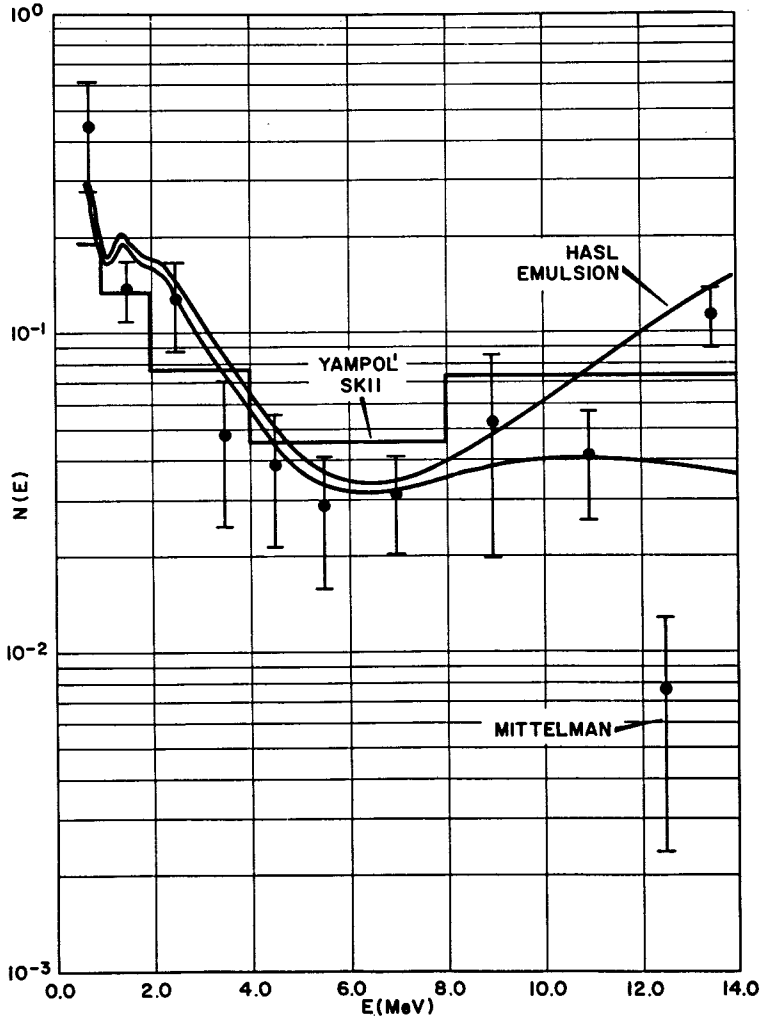

Fig. 4.4—Neutron spectrum, Emulsion # 411 (source height = 91 m, distance = 200 m, slant range = 220 m), compared with the calculations of Yampol'skii and Mittelman.

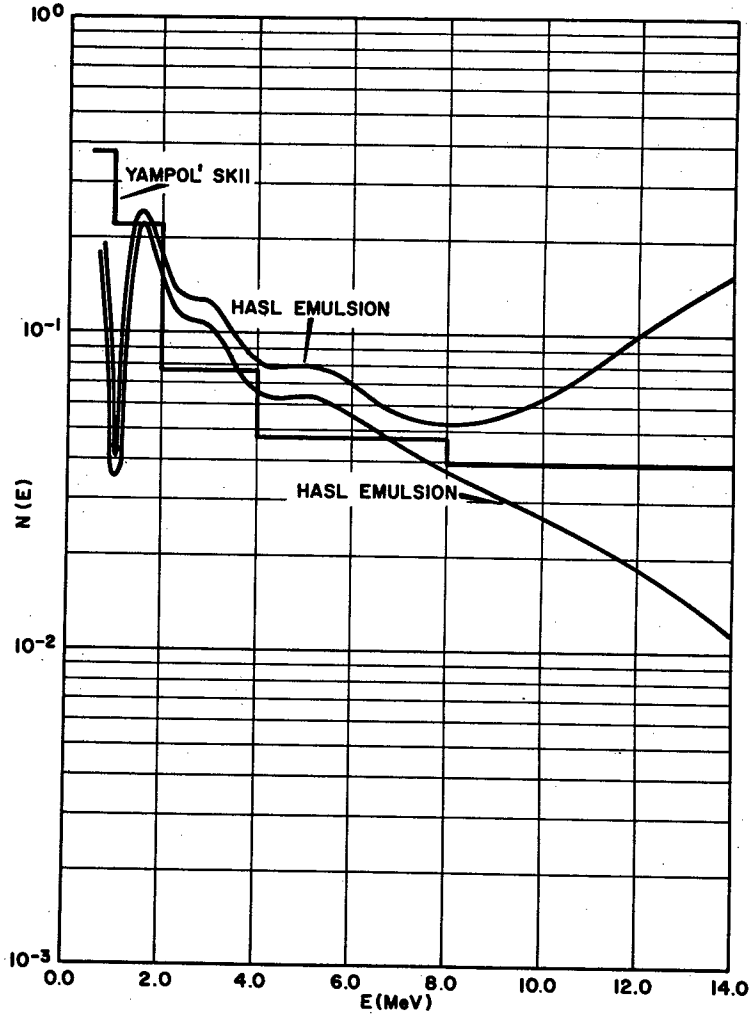

Fig. 4.5—Neutron spectrum, Emulsion # 416 (source height = 343 m, distance = 300 m, slant range = 453 m), compared with the calculations of Yampol'skii.

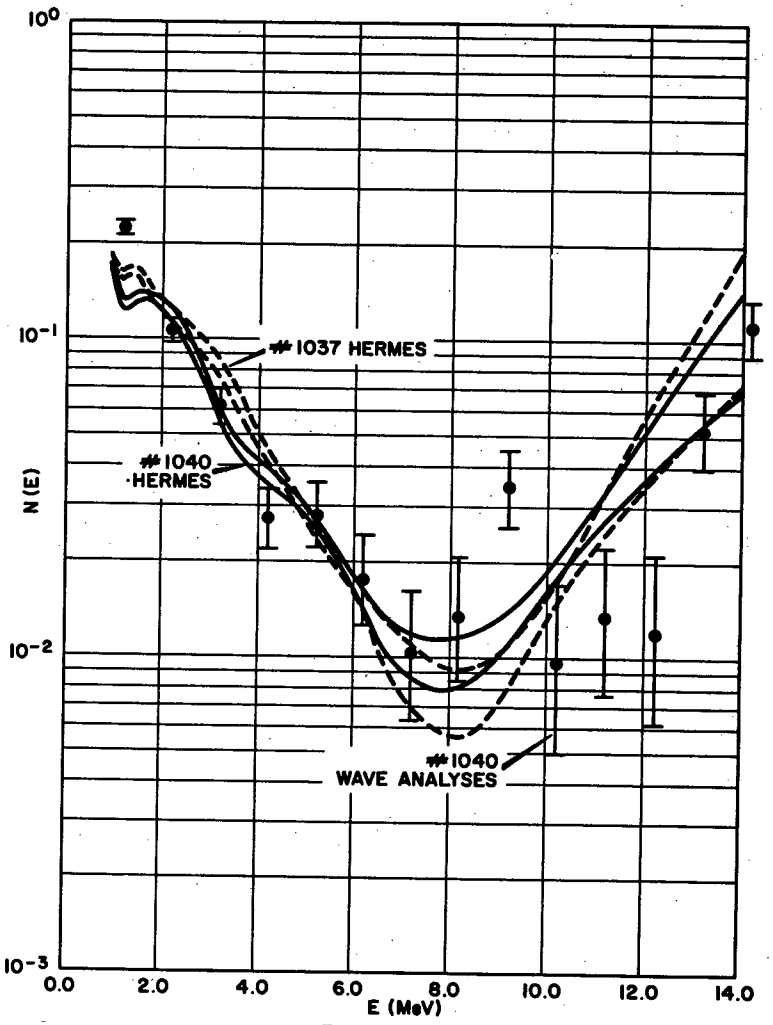

Fig. 4.6—Neutron spectra, Emulsions # 1037 and # 1040 (source height = 8.2 m, distance = 8.2 m, slant range = 11 m), with Emulsion # 1037 exposed isotropically, analyzed by HERMES and Emulsion # 1040 exposed edge-normal, analyzed both by HERMES and the plane wave method.

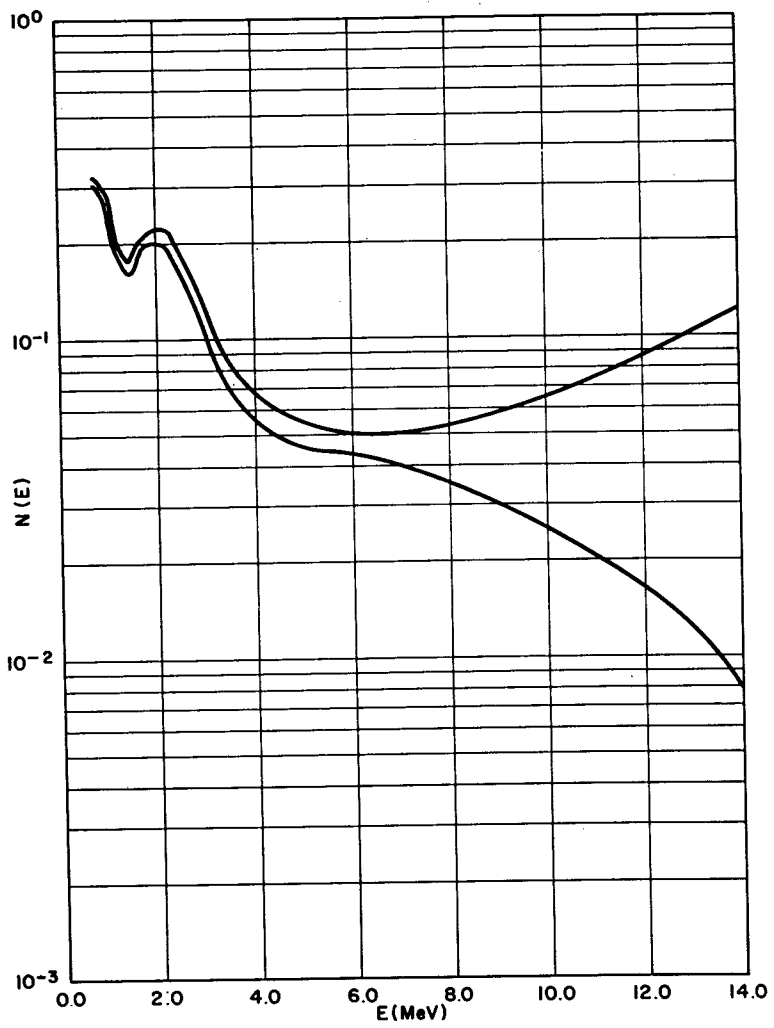

Fig. 4.7—Neutron spectrum, Emulsion # 413 (source height = 91 m, distance = 100 m, slant range = 135 m).

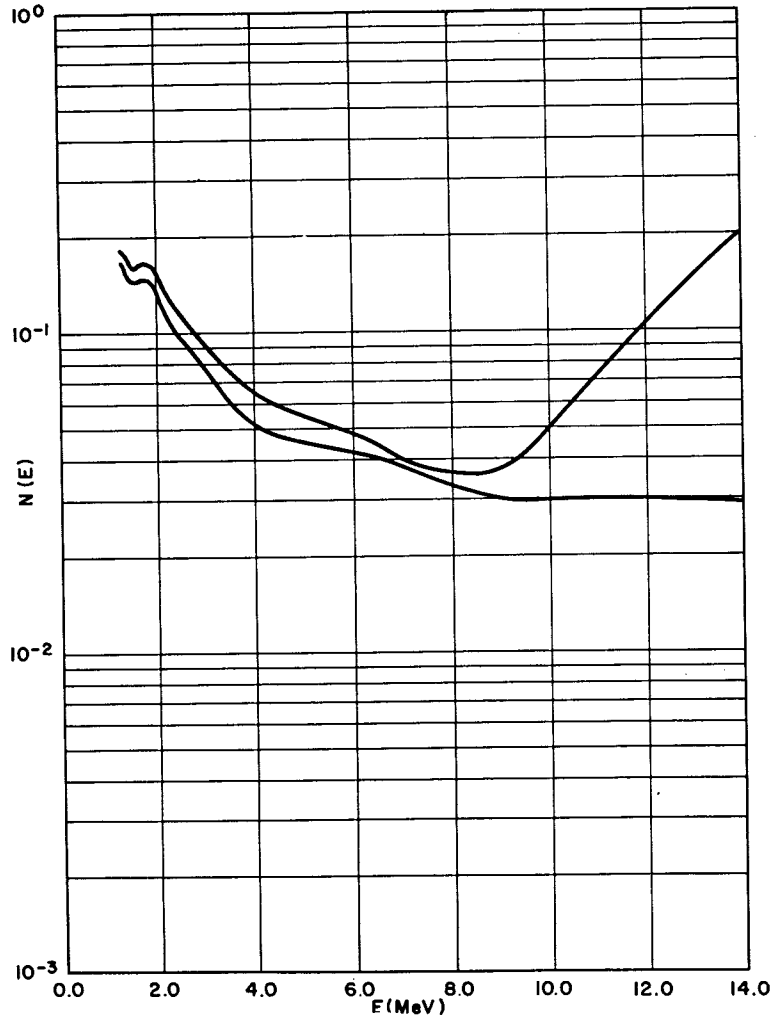

Fig. 4.8—Neutron spectrum, Emulsion # 530 (source height = 152 m, distance = 200 m, slant range = 249 m).

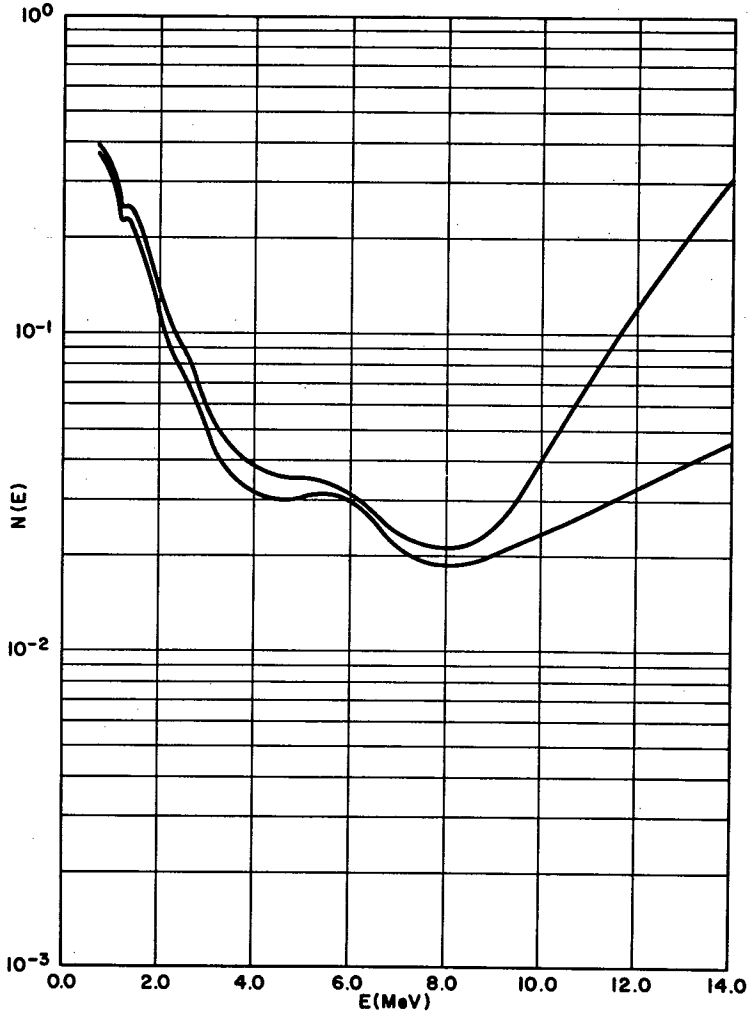

Fig. 4.9—Neutron spectrum, Emulsion # 526 (source height = 343 m, distance = 200 m, slant range = 395 m).

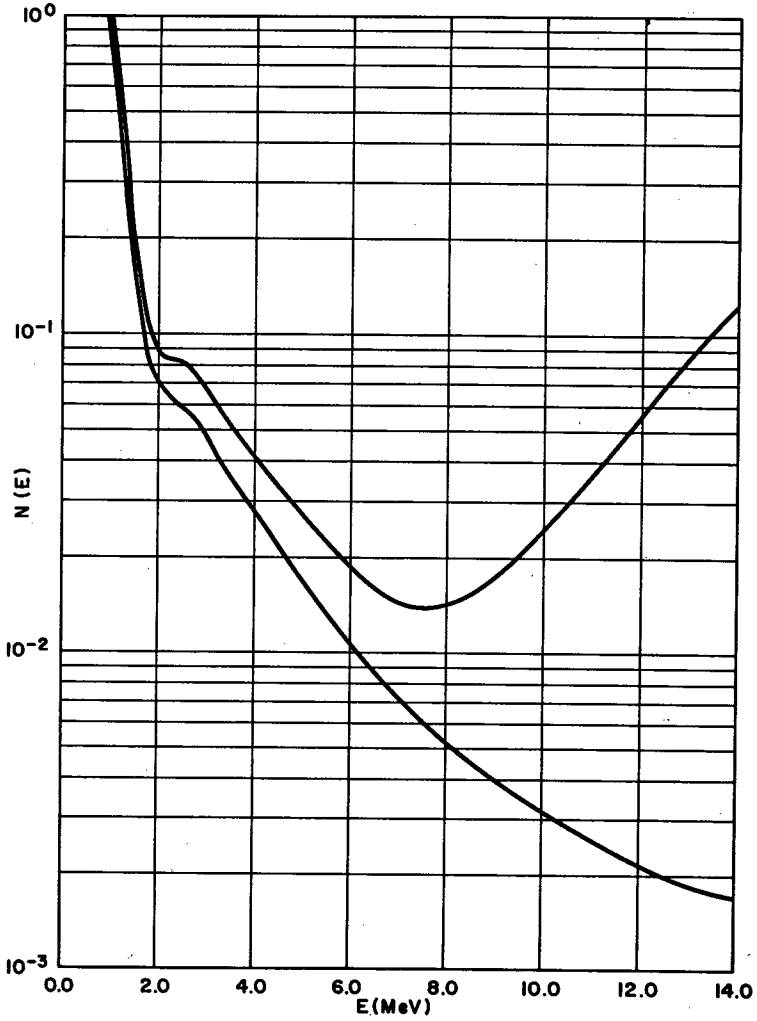

Fig. 4.10—Neutron spectrum, Emulsion # 417 (source height = 343 m, distance = 500 m, slant range = 604 m).

In Figs. 4.11 and 4.12 we show the recoil proton spectra with error bars for emulsions #406 and 417. The smooth curves are the proton spectra recalculated from the neutron spectra (shown in Figs. 4.1 and 4.10) obtained from the data by HERMES. These figures have been drawn to show what we consider a statistically good spectrum, emulsion #406, and a statistically poor one, emulsion #417. A comparison of the neutron spectra for these emulsions shows a much wider spread in the "upper and lower limits" for emulsion #417, as would be expected.

4.2 COBALT FLUX INTEGRATORS

The cobalt flux integrator measurements were normalized to unit source neutrons and are listed in Table 4.2. Straker's spectra[1] have been integrated and divided by $4\pi r^2$ to give us n/cm^2 per source neutron. The normalized fluences obtained from Straker's spectra are plotted in Fig. 4.13 versus distance in g/cm^2 with our data appearing as points with error bars. The agreement is quite good.

Finally, in Table 4.3 we report the fast neutron ($E \geq 0.75$ MeV) tissue doses for the five exposures where cobalt flux integrator and nuclear emulsion spectrometer measurements were made. To estimate the integral of the spectrum below 0.75 MeV a 1/E tail was added to the emulsion data. Knowing the specific doses D_i ($i = 1, 2, 3$ for the first collision, surface, and maximum tissue dose respectively) from Table 4.1, we calculated the fast neutron tissue doses (TD_i) for the five exposures in rads as follows:

$$TD_i = \frac{\int_{0.75}^{E_{max}} N(E)\, dE}{\int_{E_{th}}^{E_{max}} N(E)\, dE} \times D_i \times \text{Fluence}$$

where

$\int_{0.75}^{E_{max}}$ = integral of the emulsion neutron spectrum,

$\int_{E_{th}}^{E_{max}}$ = integral of emulsion neutron spectrum with a 1/E tail from thermal energy to 0.75 MeV, and

Fluence = flux integrator results (n/cm^2).

4.3 BONNER SPECTROMETRY

Figure 4.14 shows the neutron spectrum from our Bonner spectrometer exposure for a source height of 91 meters and

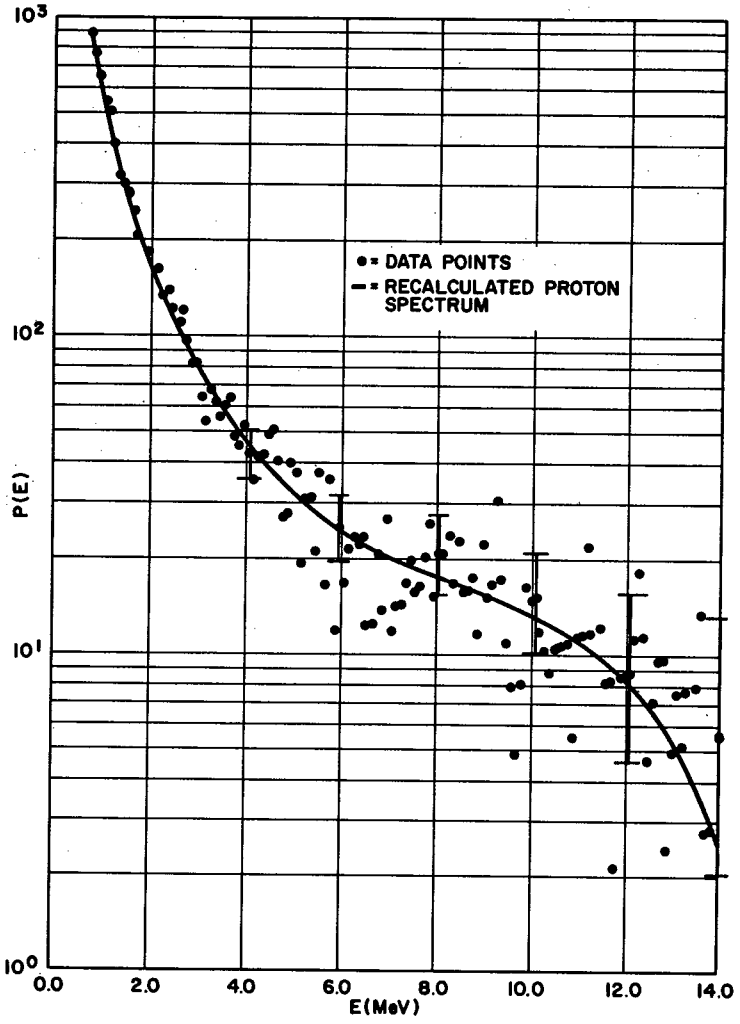

Fig. 4.11—Measured proton data points and error bars of Emulsion # 406 shown with the proton spectrum calculated from the neutron spectrum obtained by HERMES analysis of the measured data.

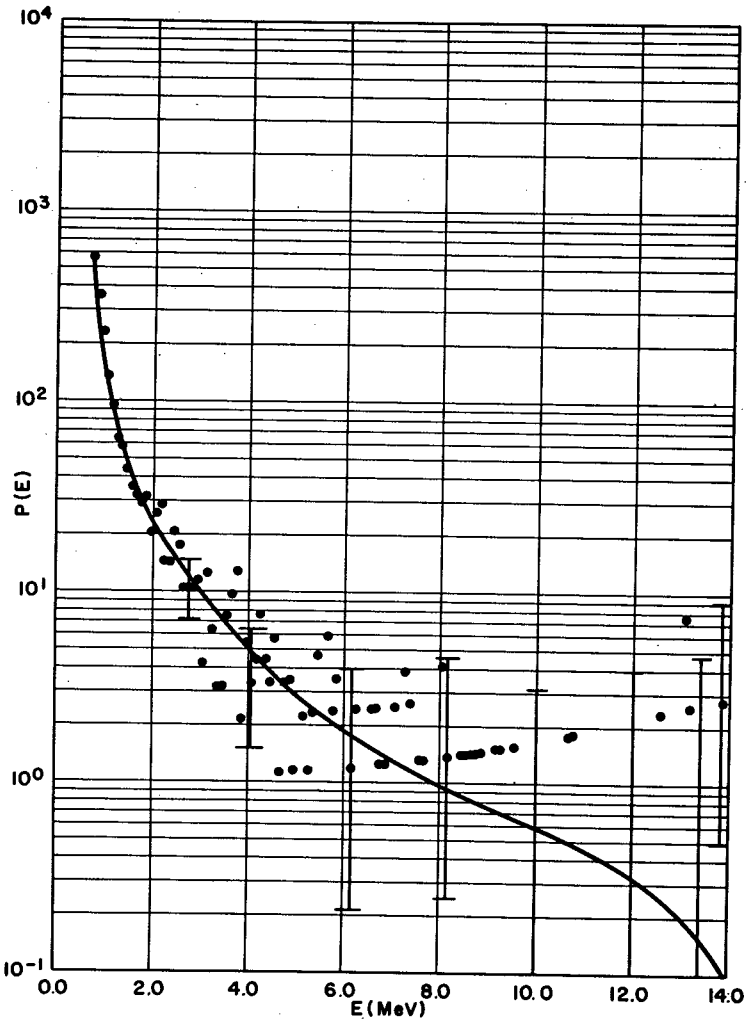

Fig 4.12—Measured proton data points and error bars of Emulsion # 417 shown with the proton spectrum calculated from the neutron spectrum obtained by HERMES analysis of the measured data.

TABLE 4.2—FLUX INTEGRATOR MEASUREMENTS

Slant range (g/cm^2)	Slant range (meters)	Source height (meters)	Distance from tower base (meters)	Neutron fluence* ($x10^7 n/cm^2$)	Source neutrons ($x10^{17} n$)	Normalized fluence* ($x10^{-10} n/cm^2$)	Emulsion No.
14.6	135	91	100	14.50±1.00	1.65	8.81±0.80	413
21.6	203	33	200	0.96±0.10	0.40	2.40±0.21	404
23.7	220	91	200	4.00±0.30	1.65	2.42±0.24	411
24.9	249	152	200	1.70±0.10	1.03	1.65±0.16	530
33.4	334	152	300	1.50±0.10	1.03	1.46±0.14	
35.6	356	343	100	1.60±0.10	1.44	1.11±0.11	
39.7	395	343	200	0.52±0.06	0.54	0.96±0.12	526
42.5	425	152	400	0.72±0.07	1.03	0.70±0.08	
52.0	520	152	500	0.39±0.06	1.03	0.38±0.06	
53.0	500	33	500	0.09±0.01	0.40	0.23±0.03	

*Data not corrected for 10 Ci ^{239}PuBe neutron source anisotropy, multiply by 1.08.

TABLE 4.3—FAST NEUTRON (E ≥ 0.75 MeV) TISSUE DOSE

Run No.	Slant range (meters)	Fluence ($x10^7 n/cm^2$)	Fluence >0.75 MeV ($x10^6 n/cm^2$)	Fast neutron dose: First collision ($x10^{-2}$ rads)	Fast neutron dose: Surface ($x10^{-2}$ rads)	Fast neutron dose: Maximum ($x10^{-2}$ rads)
12-14	203	0.96±0.1	1.57	0.7	0.92	0.97
26,27	135	14.5 ±1.0	26.7	10.8	13.6	14.6
26,27	220	4.0 ±0.3	6.76	2.8	3.7	4.0
43,44	395	0.52±0.06	0.73	0.32	0.41	0.44
48,49	249	1.7 ±0.1	6.92	3.2	4.0	4.3

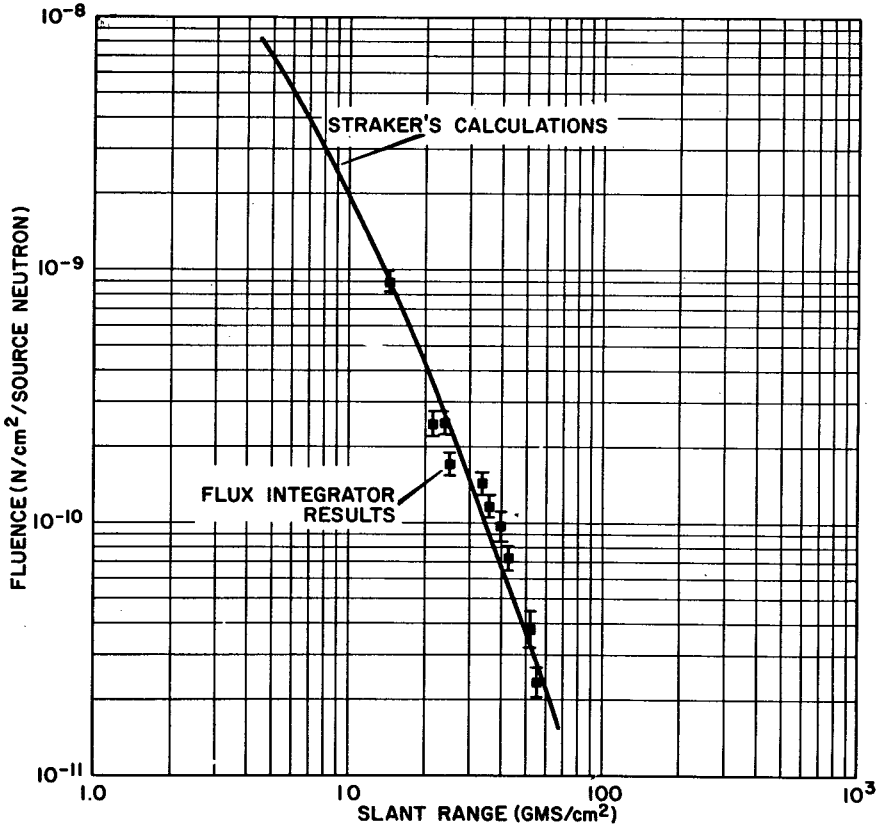

Fig. 4.13—Comparison of neutron fluences, measured with cobalt flux integrators, with fluences calculated from Straker's spectra.

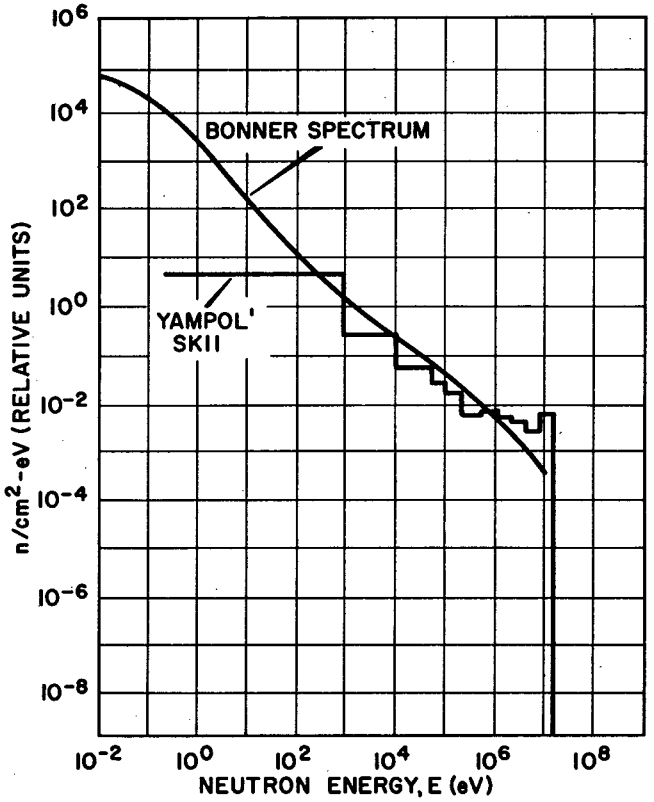

Fig. 4.14—Neutron spectrum obtained with Bonner ball spectrometer (source height = 91 m, distance = 100 m, slant range = 135 m), compared with Yampol'skii's calculations.

a distance of 100 meters. Again we compare our experimental spectra to the Yampol'skii calculation for the same slant range. The resolution of the Bonner spectrometer is very poor and little can be said of the comparison except that the curves have similar slopes. Figure 4.7 shows the emulsion spectra for the same exposure.

REFERENCES

1. E. A. Straker, "Time-Dependent Neutron and Secondary Gamma-Ray Transport in an Air-Over Ground Geometry, Volume II, Tabulated Data", USAEC Report ORNL-4289, Vol. II (September 1968).

2. E. A. Straker, "Sensitivity of Neutron Transport in Oxygen to Various Cross-Section Sets", Nucl. Sci. and Eng., 34: 332-336 (1968).

3. K. O'Brien, R. Sanna, M. Alberg, J. E. McLaughlin and S. Rothenberg, "High-Energy Accelerator Shield-Leakage Neutron Spectra", Nucl. Sci. and Eng., 27: 338-347 (1967).

4. P. A. Yampol'skii, V. E. Kokovikhin, A. I. Golubkov, N. A. Kondurushkin and A. V. Bolyatko, "Neutron Penetration in Air", Atomnaya Energiya, 21: 262-266 (October 1966).

5. P. S. Mittelman, Private Communication (1968).

Chapter 5

CONCLUSIONS

5.1 NUCLEAR TRACK EMULSIONS

The neutron spectra obtained with nuclear emulsions from the 14 MeV D-T neutron source used in Operation HENRE agree, as well as can be expected, with the available theoretical spectra. Unfortunately, we had to compare our emulsion spectra with calculations for similar, not identical, conditions. There were differences in source heights and ranges. We do feel, however, that the comparisons are valid and that the agreement is good.

Inasmuch as the emulsion measurements, as analyzed by our program HERMES, give a low resolution spectrum, we could not satisfactorily resolve the peak at 2.37 MeV in the HENRE spectra although the inflection in our data indicates the existence of such a peak. Of course, we have been able to resolve the major D-T source peak at 14 MeV.

Another technique used for this type of spectrometry was to expose the emulsions edge-on and to do a plane wave geometry analysis of the data. Unfortunately, to get a statistically reliable spectrum with this technique, a vast quantity of data must be analyzed. As can be seen in Fig. 4.6 even 15,000 tracks are not enough. This is because the vast majority of the acceptable data is under the 14 MeV peak and at the low energy end, which makes it necessary to collect great quantities of data to get meaningful results in the energy range of 5 - 12 MeV.

Therefore, one may conclude that both HERMES and the plane wave method of analysis have advantages and drawbacks and it is necessary to study each experiment, weighing the information sought, the kind of spectra likely to be encountered, etc. before deciding which method of analysis is most suitable. For the type of spectra encountered during Operation HENRE, the HERMES analysis, despite its lower resolution, is the most suitable because a reasonable representation of the neutron spectrum can be obtained from

much less data than are necessary for the plane wave method of analysis.

During Operation HENRE we had an excellent opportunity to test our procedures in emulsion spectroscopy and problems arising during the experiment have resulted in improvements in our procedures. Detailed analysis of the statistical accuracy of the data of individual scanners and of the neutron spectrum as a whole resulted from this work. We feel that our participation in HENRE made us much more knowledgeable in the proper use of nuclear emulsions as a neutron spectrometer.

5.2 COBALT FLUX INTEGRATORS

The cobalt flux integrator measurements agree quite well with Straker's data (Fig. 4.13). Again the comparisons are not for identical situations. Straker's calculations are for a 54 foot source height (16.5 m), our measurements were obtained for source heights ranging from 33 m to 343 m. The results lead us to conclude that until better response data are available for the flux integrator, the use of the response data interpolated from the Bonner spectrometer response functions, as described in section 3.2, is a reasonable approximation.

The use of a 1/E tail on our emulsion spectra in determining the fast neutron tissue dose is felt to be reasonable. We have not reported error estimates for the fluences above 0.75 MeV or for the fast neutron doses (Table 4.3) because we do not know what error is actually involved in assuming the 1/E tail. The results, however, are probably good within a factor of 2.

5.3 BONNER SPECTROMETRY

The spectrum obtained using the Bonner spectrometer and its agreement with the calculated spectrum of Yampol'skii (Fig. 4.14) give us reason to believe that this spectrometer can be of use to obtain low resolution neutron spectra from thermal energies to about 10 MeV. A great deal of work is still needed in the error analysis of data obtained with this spectrometer and more experience with the actual use of the Bonner spectrometer to measure neutron spectra is necessary. When such experience is obtained, it may prove of particular value in health physics in developing low resolution neutron spectra and values for specific tissue doses.

CIVIL EFFECTS TEST OPERATIONS REPORT SERIES (CEX)

Through its Division of Biology and Medicine and Civil Effects Test Operations, the Atomic Energy Commission conducts certain technical tests, exercises, surveys, and research directed primarily toward practical applications of nuclear effects information and toward encouraging better technical, professional, and public understanding and utilization of the vast body of facts useful in the design of countermeasures against weapons effects. The activities carried out in these studies do not require nuclear detonations.

The following is a partial list of reports available from studies that have been completed. All reports listed are available, at $3.00 each, from the Clearinghouse for Federal Scientific and Technical Information, U. S. Department of Commerce, Springfield, Va. 22151.

CEX-58.1, Experimental Evaluation of the Radiation Protection Afforded by Residential Structures Against Distributed Sources, J. A. Auxier, J. O. Buchanan, C. Eisenhauer, and H. E. Menker, 1959.

CEX-58.7, AEC Group Shelter, AEC Facilities Division, Holmes & Narver, Inc., 1960.

CEX-58.8, Comparative Nuclear Effects of Biomedical Interest, C. S. White, I. G. Bowen, D. R. Richmond, and R. L. Corsbie, 1961.

CEX-58.9, A Model Designed to Predict the Motion of Objects Translated by Classical Blast Waves, I. G. Bowen, R. W. Albright, E. R. Fletcher, and C. S. White, 1961.

CEX-59.1, An Experimental Evaluation of the Radiation Protection Afforded by a Large Modern Concrete Office Building, J. F. Batter, Jr., A. L. Kaplan, and E. T. Clarke, 1960.

CEX-59.7B (Pt. I), Experimental Radiation Measurements in Conventional Structures. Part I. Radiation Measurements in Two Two-story and Three One-story Typical Residential Structures Before and After Modification, Z. G. Burson, 1966.

CEX-59.7B (Pt. II), Experimental Radiation Measurements in Conventional Structures. Part II. Comparison of Measurements in Above-ground and Below-ground Structures from Simulated and Actual Fallout Radiation, Z. G. Burson, 1964.

CEX-59.7B (Pt. III), Experimental Radiation Measurements in Conventional Structures. Part III. The Attenuation of Air-scattered Radiation in a Basement, Z. G. Burson, 1965.

CEX-59.13, Experimental Evaluation of the Radiation Protection Afforded by Typical Oak Ridge Homes Against Distributed Sources, T. D. Strickler and J. A. Auxier, 1960.

CEX-59.14, Determinations of Aerodynamic-drag Parameters of Small Irregular Objects by Means of Drop Tests, E. P. Fletcher, R. W. Albright, V. C. Goldizen, and I. G. Bowen, 1961.

CEX-60.1, Evaluation of the Fallout Protection Afforded by Brookhaven National Laboratory Medical Research Center, H. Borella, Z. Burson, and J. Jacovitch, 1961.

CEX-60.3, Extended- and Point-source Radiometric Program, F. J. Davis and P. W. Reinhardt, 1962.

CEX-60.5, Experimental Evaluation of the Fallout-radiation Protection Afforded by a Southwestern Residence, Z. Burson, D. Parry, and H. Borella, 1962.

CEX-60.6, Experimental Evaluation of the Radiation Protection Provided by an Earth-covered Shelter, Z. Burson and H. Borella, 1962.

CEX-61.1 (Prelim.), Gamma Radiation at the Air–Ground Interface, K. O'Brien and J. E. McLaughlin, Jr., 1963.

CEX-61.4, Experimental Evaluation of the Fallout-radiation Protection Provided by Selected Structures in the Los Angeles Area, Z. G. Burson, 1963.

CEX-62.01, Technical Concept—Operation BREN, J. A. Auxier, F. W. Sanders, F. F. Haywood, J. H. Thorngate, and J. S. Cheka, 1962.

CEX-62.2, Nuclear Bomb Effects Computer (Including Slide-rule Design and Curve Fits for Weapons Effects), E. R. Fletcher, R. W. Albright, R. F. D. Perret, Mary E. Franklin, I. G. Bowen, and C. S. White, 1963.

CEX-62.11, Distribution of Weapons Radiation in Japanese Residential Structures, J. S. Cheka, F. W. Sanders, T. D. Jones, and W. H. Shinpaugh, 1965.

CEX-62.12, Energy and Angular Distribution of Neutrons and Gamma Rays—Operation BREN, J. H. Thorngate, J. A. Auxier, F. F. Haywood, and S. Helf, 1967.

CEX-62.13, Post Pulse Gamma-radiation Spectrum—Operation BREN, J. H. Thorngate and E. T. Loy, 1966.

CEX-62.14, An Experimental Investigation of the Spatial Distribution of Dose in an Air-over-Ground Geometry, F. F. Haywood, J. A. Auxier, and E. T. Loy, 1964.

CEX-62.50, Neutron-field and Induced-activity Measurements—Operation BREN, F. M. Tomnovec and J. M. Ferguson, 1965.

CEX-62.80b, Small Boy Project 62.80b Aeroradioactivity Survey, Edgerton, Germeshausen & Grier, Inc., 1967.

CEX-62.80c, Sedan Project 62.80c Aeroradioactivity Survey, Edgerton, Germeshausen & Grier, Inc., 1967.

CEX-62.81 (Final), Ground Roughness Effects on the Energy and Angular Distribution of Gamma Radiation from Fallout, C. M. Huddleston, Z. G. Burson, R. M. Kinkaid, and Q. G. Klinger, 1964.

CEX-63.3, Barrier Attenuation of Air-scattered Gamma Radiation, Z. G. Burson and R. L. Summers, 1965.

CEX-63.7, A Comparative Analysis of Some of the Immediate Environmental Effects at Hiroshima and Nagasaki, C. S. White, I. G. Bowen, and D. R. Richmond, 1964.

CEX-63.10, Design of a Shielded Source for the Irradiation of Natural Animal Populations, A. C. Lucas, Z. G. Burson, and R. E. Lagerquist, 1966.

CEX-64.3, Ichiban: The Dosimetry Program for Nuclear Bomb Survivors of Hiroshima and Nagasaki—A Status Report as of April 1, 1964, J. A. Auxier, 1964.

CEX-64.7, Neutron and Gamma-ray Leakage from the Ichiban Critical Assembly, J. H. Thorngate, D. R. Johnson, and P. T. Perdue, 1966.

CEX-65.01, Feasibility Study: Intense 14-Mev Neutron Source for Operation HENRE, T. G. Provenzano, E. J. Story, F. F. Haywood, and H. T. Miller, 1966.

CEX-65.02, Technical Concept—Operation HENRE, F. F. Haywood and J. A. Auxier, 1965.

CEX-65.03, Operations Plan—Operation HENRE, Technical Director's Staff, 1965.

CEX-65.4, Biological Tolerance to Air Blast and Related Biomedical Criteria, C. S. White, I. Gerald Bowen, and D. R. Richmond, 1965.

CEX-65.11, Energy and Angular Distribution of Neutrons and Gamma Rays—Operation BREN, J. H. Thorngate, D. R. Johnson, and P. T. Perdue, 1969.

CEX-65.13, Distribution of Radiation from a 14 Mev Neutron Source in and Near Structures, J. S. Cheka, 1969.

CEX-68.3, Nuclear Weapons Effects Tests of Blast Type Shelters, A Documentary Compendium of Test Reports, Christian Beck (Comp.), 1969.

CEX-68.4, Radiosensitivity of Certain Perennial Shrub Species Based on a Study of the Nuclear Excavation Experiment, Palanquin, with Other Observations of Effects on the Vegetation, W. A. Rhoads, Robert B. Platt, and Robert A. Harvey, 1969.